Int. J. Solids Structures Vol. 21, No. 12, pp. 1165–1179, 1985
Printed in Great Britain.

0020-7683/85 $3.00 + .00
© 1985 Pergamon Press Ltd.

THE STRESS FIELD OF A SLIDING INCLUSION

T. MURA, I. JASIUK and B. TSUCHIDA†
Department of Civil Engineering and Materials Research Center, The Technological Institute, Northwestern University, Evanston, Illinois 60201, U.S.A.

(*Received* 4 *June* 1984; *in revised form* 18 *January* 1985)

Abstract—This paper discusses the stress fields when a spheroidal inclusion, free to slip along its interface, is subjected to a constant nonshear eigenstrain, and when an elastic body containing the inhomogeneity is under all-around tension or uniaxial tension at infinity. In each case the stress field in the inclusion or the inhomogeneity is not constant, contrary to Eshelby's solution. When sliding takes place, the stress increases locally compared with the perfect bonding case, but the elastic energy decreases due to the relaxation. The relative displacement (slip) along the interface is also evaluated.

1. INTRODUCTION

When an ellipsoidal subdomain in an infinite body is subjected to a uniform eigenstrain (transformation strain, thermal strain, plastic strain, etc.), the resulting stress field is called an eigenstress field, and the subdomain is called an ellipsoidal inclusion.

When an ellipsoidal subdomain in an infinite body has different elastic moduli from those of the remainder (matrix) and is subjected to a uniform applied stress at infinity, the resulting stress field is the sum of the uniform stress and a stress disturbance. The subdomain is called an ellipsoidal inhomogeneity.

These two problems (the eigenstress and the stress disturbance) are essentially the same problems (mathematically) and are called the inclusion problems. The inclusion problems have been investigated by many researchers: Goodier[1], Sadowsky and Sternberg[2], Miyamoto[3], Edwards[4], Eshelby[5, 6], Walpole[7], Kinoshita and Mura[8] and Asaro and Barnett[9], among others. Most papers, however, are based on the assumption that the inclusion or the inhomogeneity and the matrix are perfectly bonded, i.e.

$$[\sigma_{ij}]n_j = 0 \qquad \text{on S}, \tag{1}$$

and

$$[u_i] = 0 \qquad \text{on S}, \tag{2}$$

where $[\ ] \equiv$ (out)–(in) and n_i is the normal vector on surface S. The first condition is the continuity of interfacial tractions across the interface, and the second condition is the continuity of displacements across S.

Most inclusions and inhomogeneities in real materials, however, are not perfectly bonded. Grains in polycrystals, particles in soils, and fibers in composite materials, for instance, are subjected to sliding along the interfaces.

In this paper the condition (2) is relaxed to

$$[u_i]n_i = 0. \tag{3}$$

This condition means that the displacement component normal to S is continuous, but the displacement component tangential to S can be discontinuous. Also, the assumption is made that the shear tractions vanish along the interface.

Recently Mura and Furuhashi[10] have obtained a striking result for the sliding inclusion. They found that when an ellipsoidal inclusion undergoes a shear eigenstrain

† Faculty of Engineering, Saitama University, 255 Shimo-Okubo, Urawa, Japan.

and the inclusion is free to slip along the interface, the stress field vanishes everywhere in the inclusion and the matrix. This result indicates that if the inclusion is free to slip, no back stress is accumulated by this local eigenstrain and no resistance for shear deformation is expected. This is not true, however, when the eigenstrain is not of shear type as considered in this analysis.

The case for a sliding spherical inhomogeneity under tension at infinity has already been investigated by Ghahremani[11].

In this paper we investigate a prolate spheroidal inclusion with nonshear-type eigenstrain ϵ_{ij}^{*}. We also study a prolate spheroidal inhomogeneity under all-around tension (plane hydrostatic state of stress) or uniaxial tension (along the major axis of a prolate spheroid) at infinity. These problems can be approached by the same method of Boussinesq using infinite series of displacement potentials which have already been used by Tsuchida and Mura[12] for the problem of inhomogeneity in a half space. The analysis is similar to that of Edwards[4], but it is modified such that the method is easily applied to the half-space problems and the problems with more general boundary conditions.

2. METHOD OF SOLUTION

Consider an isotropic and infinitely extended elastic body, containing a prolate spheroidal subdomain that may have elastic constants different from those of the matrix, as shown in Fig. 1.

The present problem is to solve the stress fields caused by all-around tension at infinity (Fig. 1), uniaxial tension at infinity or by uniform nonshear eigenstrains in the inclusion. In each case the inhomogeneity or the inclusion can slide along the interface and the tangential shear forces vanish on the interface. The method of analysis is applicable for each loading condition.

We follow the method developed by Sadowsky and Sternberg[2] and Edwards[4]. However, the modifications are made so the analysis can be extended to a wider range of problems.

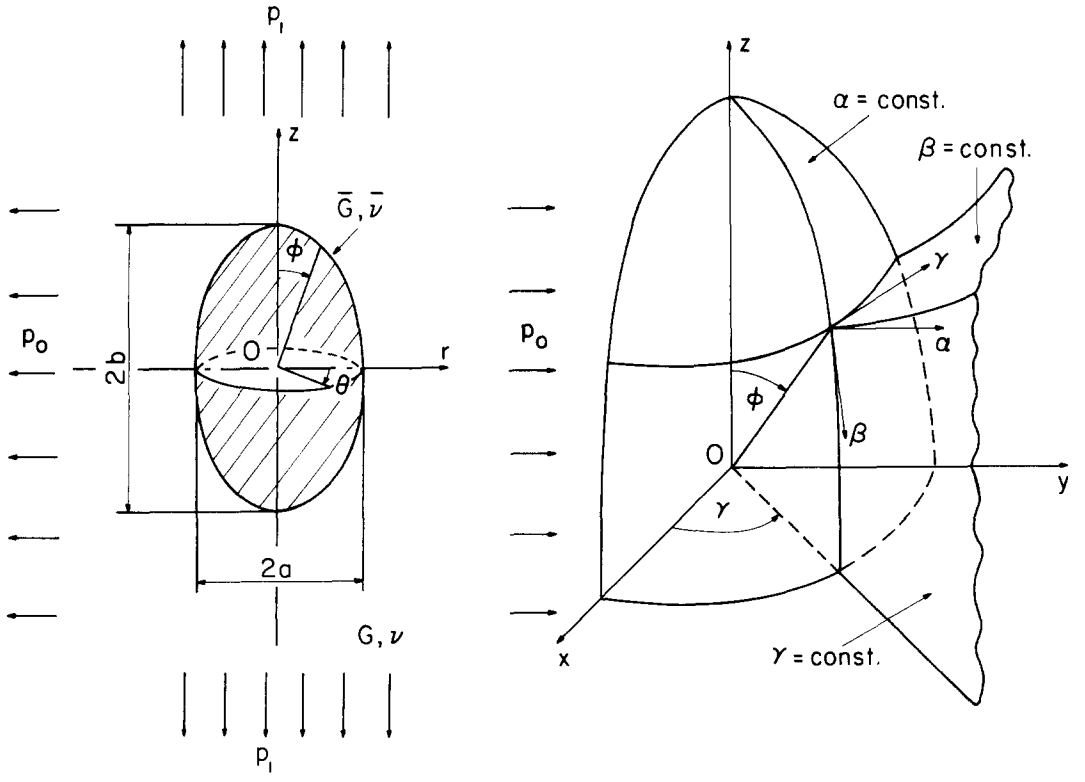

Fig. 1. Coordinate system.

Let the origin of coordinates 0 be at the center of the inhomogeneity or the inclusion and $0Z$ coincide with the axis of symmetry of the configuration. The prolate spheroidal coordinate system (α, β, γ) is related to Cartesian (x, y, z) by the transformation equation:

$$\begin{aligned} x &= c \sinh \alpha \sin \beta \cos \gamma \\ y &= c \sinh \alpha \sin \beta \sin \gamma \\ z &= c \cosh \alpha \cos \beta, \end{aligned} \tag{4}$$

where c is the focal distance in the prolate direction (the z axis direction). Sadowsky and Sternberg[2] and Edwards[4] take $c = 1$. Tsuchida and Mura[12] keep c as a constant. The advantage to the second approach is that the analysis can be extended to the half-space problem, where the distance from the center of the ellipsoid to the surface of half-space is taken as unity. Then we can choose the Boussinesq's potential functions as the product of the ordinary Legendre functions of the first and the second kinds, derived from the integral of the product $e^{\lambda z} J_0(\lambda r)$, that will satisfy the boundary conditions at $z = -1$ (see [12]).

From eqn (4) the differential of arc length is written in the form

$$(ds)^2 = (d\alpha/h)^2 + (d\beta/h)^2 + (d\gamma/h_3)^2, \tag{5}$$

where

$$h = 1/c(q^2 - p^2)^{1/2}, \qquad h_3 = 1/c\bar{q}\bar{p} \tag{6}$$

with

$$\begin{aligned} q &= \cosh \alpha, \qquad \bar{q} = \sinh \alpha \\ p &= \cos \beta, \qquad \bar{p} = \sin \beta. \end{aligned} \tag{7}$$

The ranges of these variables are

$$\begin{aligned} 1 \leqq q < \infty, \qquad & 0 \leqq \bar{q} < \infty, \\ -1 \leqq p \leqq 1, \qquad & 0 \leqq \bar{p} \leqq 1. \end{aligned} \tag{8}$$

The surface of the ellipsoid is defined by $\alpha = \alpha_0$ or the corresponding variable $q_0 = \cosh \alpha_0$. The minor and major semi-axes of the spheroid are defined by

$$a = c\bar{q}_0, \qquad b = cq_0. \tag{9}$$

The displacement components in the Cartesian coordinate system are expressed by the Boussinesq's potential functions ψ, ϑ and λ in the particular formulation employed by Sadowsky and Sternberg[2]

$$\begin{aligned} [u, v, w] &= \frac{1}{2G} \operatorname{grad} \psi, \\ [u, v, w] &= \frac{1}{G} \operatorname{curl}[0, 0, \vartheta] \\ [u, v, w] &= \frac{z}{2G} \operatorname{grad} \lambda - \left[0, 0, \frac{3 - 4\nu}{2G} \lambda\right] \end{aligned} \tag{10}$$

where G and ν are the shear modulus and Poisson's ratio, respectively. When the expression (10) is applied to the inclusion or the inhomogeneity, G and ν are taken as $\bar{G}$ and $\bar{\nu}$.

The slip boundary conditions at the interface of the inclusion, i.e. at $\alpha = \alpha_0$ are

$$\begin{aligned} u_\alpha &= \bar{u}_\alpha, \qquad \sigma_\alpha = \bar{\sigma}_\alpha, \\ \tau_{\alpha\beta} &= 0, \qquad \bar{\tau}_{\alpha\beta} = 0, \end{aligned} \tag{11}$$

In the above expressions, quantities referring to the inclusion (or inhomogeneity) are denoted by a bar. Because we are considering the symmetrical problems about the z axis, $\tau_{\gamma\alpha}$ and $\tau_{\gamma\beta}$ must vanish everywhere.

The boundary conditions at infinity are

$$\sigma_x = \sigma_y = p_0, \qquad \alpha \to \infty \tag{12}$$

for the all-around tension case,

$$\sigma_z = p_1, \qquad \alpha \to \infty \tag{13}$$

for the uniaxial tension along the z axis, and

$$\begin{aligned} \sigma_\alpha &= \sigma_\beta = \sigma_\gamma = 0, \\ \tau_{\alpha\beta} &= 0, \qquad \alpha \to \infty \end{aligned} \tag{14}$$

for the eigenstrain problem, where the inclusion can be also an inhomogeneity. The nonshear eigenstrain components ϵ_x^*, ϵ_y^*, ϵ_z^* are considered and

$$\epsilon_x^* = \epsilon_y^* \tag{15}$$

because of the symmetry about the z axis. The displacements inside the inclusion are the sum of the free deformation given by

$$u^* = \epsilon_x^* x, \qquad v^* = \epsilon_y^* y, \qquad w^* = \epsilon_z^* z \tag{16}$$

and the displacements obtained from eqn (10).

The stress and displacement components expressed in the prolate spheroidal coordinate system can be easily obtained by dimensional analysis from Edwards' result[4] by multiplying his expressions by c, c^{-1} or c^2 as needed. For instance, ψ/G must have the dimension cm^2, q, $\bar{q}$, p, $\bar{p}$, γ have no dimension and h has the dimension $(\text{cm})^{-1}$. Therefore, Edwards' expression $u_\gamma = \psi_\gamma/2G\bar{p}\bar{q}$ must be changed to $u_\gamma = \psi_\gamma/2Gc\bar{p}\bar{q}$ and $u_\alpha = h\bar{q}\psi_q/2G$ is left unchanged. The stress term $h^4\bar{p}^2q\psi_q$ must be changed to $c^2h^4\bar{p}^2q\psi_q$.

The stress fields and the associated displacement fields can be transformed from the Cartesian coordinate system into prolate spheroidal coordinate system by using the transformation coefficients listed in Table 1.

After eqn (10) is transformed into prolate spheroidal coordinates the displacement

Table 1

	x	y	z
α	$ch\bar{q}\bar{p}\cos\gamma$	$ch\bar{q}\bar{p}\sin\gamma$	$ch\bar{q}p$
β	$ch\bar{q}p\cos\gamma$	$ch\bar{q}p\sin\gamma$	$-ch\bar{q}\bar{p}$
γ	$-\sin\gamma$	$\cos\gamma$	0

and the stress disturbances due to inhomogeneity or the inclusion are determined from (10) by choosing the following potential functions:

$$\psi = C_0 \sum_{n=0}^{\infty} A_n Q_n(q) P_n(p),$$
$$\lambda = C_0 \sum_{n=0}^{\infty} B_n Q_n(q) P_n(p) \tag{17}$$

for the matrix ($\alpha > \alpha_0$) and

$$\psi = C_0 \sum_{n=0}^{\infty} \bar{A}_n P_n(q) P_n(p),$$
$$\lambda = C_0 \sum_{n=0}^{\infty} \bar{B}_n P_n(q) P_n(p) \tag{18}$$

for the inclusion ($\alpha < \alpha_0$), where

$$C_0 = \begin{cases} p_0 & \text{for all-around tension,} \\ p_1 & \text{for uniaxial tension,} \\ 2G\epsilon_x^* \text{ or } 2G\epsilon_z^* & \text{for eigenstrain case,} \end{cases} \tag{19}$$

and $P_n(p)$ and $Q_n(q)$ are the Legendre functions of the first and second kinds, respectively. The explicit expressions for $P_n(p)$ and $Q_n(q)$ are

$$P_n(p) = \frac{1}{2^n n!} \frac{d^n}{dp^n} (p^2 - 1)^n,$$
$$Q_n(q) = \tfrac{1}{2} P_n(q) \log \frac{q+1}{q-1} - W_{n-1}(q) \tag{20}$$

where

$$W_{n-1}(q) = \frac{2n-1}{1(n)} P_{n-1}(q) + \frac{2n-5}{3(n-1)} P_{n-3}(q) + \frac{2n-9}{5(n-2)} P_{n-5}(q) + \cdots .$$

The series ends when the index m of P_m becomes negative.

The undisturbed displacement and stress fields before introduction of the inclusion analyzed in this paper are transformed into spheroidal coordinates and expressed in terms of ordinary Legendre function $P_n(p)$. The undisturbed displacement u_α and stresses σ_α and $\tau_{\alpha\beta}$ needed for the continuity equations are as follows:

For all-around tension ($\sigma_x = \sigma_y = p_0$)

$$\frac{2Gu_\alpha}{p_0} = h\bar{q} \left\{ c^2 q \frac{2}{3} \left[\frac{(1-2\nu)}{1+\nu} P_0(p) - P_2(p) \right] \right\},$$
$$\frac{\sigma_\alpha}{p_0} = c^2 h^4 \{ c^2 q^2 [(\tfrac{2}{3}q^2 - \tfrac{2}{15}) P_0(p) - (\tfrac{2}{21} + \tfrac{2}{3}q^2) P_2(p) + \tfrac{8}{35} P_4(p)] \}, \tag{21}$$
$$\frac{\tau_{\alpha\beta}}{p_0} = c^2 h^4 \bar{q}\bar{p} \{ c^2 q [(\tfrac{1}{3}q^2 - \tfrac{1}{7}) P_2'(p) - \tfrac{2}{35} P_4'(p)] \},$$

for uniaxial tension ($\sigma_z = p_1$)

$$\frac{2Gu_\alpha}{p_1} = h\bar{q}\left\{c^2 q\left[\frac{1-2\nu}{3(1+\nu)}P_0(p) + \tfrac{2}{3}P_2(p)\right]\right\},$$

$$\frac{\sigma_\alpha}{p_1} = c^2h^4\{c^2\bar{q}^2[(\tfrac{1}{3}q^2 - \tfrac{1}{5})P_0(p) + (\tfrac{2}{3}q^2 - \tfrac{4}{7})P_2(p) - \tfrac{8}{35}P_4(p)]\}, \tag{22}$$

$$\frac{\tau_{\alpha\beta}}{p_1} = c^2h^4\bar{q}\bar{p}\{c^2q[(\tfrac{1}{7} - \tfrac{1}{3}q^2)P_2'(p) + \tfrac{2}{35}P_4'(p)]\},$$

and for eigenstrain case

$$\frac{2G\bar{u}_\alpha}{C_0} = \frac{h\bar{q}}{C_0}\left\{c^2q\frac{2G}{3}[(2\epsilon_x^* + \epsilon_z^*)P_0(p) + 2(\epsilon_z^* - \epsilon_x^*)P_2(p)]\right\} \tag{23}$$

where $P_n'(p)$ is the derivative of $P_n(p)$.

These stresses and displacements due to the loading conditions are combined with the stresses and displacements due to the inhomogeneity or the inclusion derived from eqns (17) and (18) and are substituted in the continuity equations (11). The unknown constants A_n, B_n, $\bar{A}_n$, $\bar{B}_n$ are determined by comparing the coefficients of $P_n(p)$ or $P_n'(p)$ in eqn (11). It is found that $A_n(n = 1, 3, 5, \ldots)$, $B_n(n = 0, 2, 4, \ldots)$, $\bar{A}_n(n = 1, 3, 5, \ldots)$ and $\bar{B}_n(n = 0, 2, 4, \ldots)$ are zero because the stresses are symmetrical about the z axis.

3. ELASTIC STRAIN ENERGY

The potential energy change ΔW of the inhomogeneity from the uniform stress field and the elastic strain energy W of the inclusion due to eigenstrains are important quantities to investigate the relaxation effect of slip and the macroscopic elastic modulus of composite materials when the self-consistent method is applied.

When a sliding inclusion undergoes a uniform eigenstrain, the elastic strain energy is expressed as

$$W = \frac{1}{2}\iiint_D \sigma_{ij}(u_{i,j} - \epsilon_{ij}^*)\,dV. \tag{24}$$

The integration domain D is the sum of domains of matrix $D - \Omega$ and inclusion Ω. On the other hand, we have

$$\iiint_{D-\Omega} \sigma_{ij}u_{i,j}\,dV = \iint_{|D|} \sigma_{ij}n_ju_i\,dS - \iint_{|\Omega|} \sigma_{ij}n_ju_i(\text{out})\,dS \tag{25}$$

where $|D|$ is the boundary of D which is at infinity and $|\Omega|$ is that of Ω, and $\mathbf{n}$ is the outer normal to the surface element dS.

We have also

$$\iiint_{\Omega} \sigma_{ij}u_{i,j}\,dV = \iint_{|\Omega|} \sigma_{ij}n_ju_i(\text{in})\,dS. \tag{26}$$

The sum of eqns (25) and (26) is

$$\iiint_{D} \sigma_{ij}u_{i,j}\,dV = -\iint_{|\Omega|} \sigma_{ij}n_j[u_i]\,dS, \tag{27}$$

since $\sigma_{ij}n_j = 0$ on $|D|$, where $[u_i] = u_i(\text{out}) - u_i(\text{in})$.

The force traction $\sigma_{ij}n_j$ is continuous and has no shear component along the interface $|\Omega|$. Since $\sigma_{ij}n_j$ has no tangential shear component, $\sigma_{ij}n_j[u_i]$ vanishes along the interface. Therefore eqn (24) becomes

$$W = -\frac{1}{2}\iiint_{\Omega} \sigma_{ij}\epsilon^*_{ij}\,dV. \tag{28}$$

When a sliding inhomogeneity is subjected to an applied stress σ^0_{ij} at infinity, the potential energy is expressed as

$$W = \frac{1}{2}\iiint_{D} (\sigma^0_{ij} + \sigma_{ij})(u^0_{i,j} + u_{i,j})\,dV - \iint_{|D|} \sigma^0_{ij}n_j(u^0_i + u_i)\,dS, \tag{29}$$

where u^0_i is the homogeneous displacement when no inhomogeneity exists under σ^0_{ij}. The potential energy of the system before introduction of the inhomogeneity is

$$W_0 = \frac{1}{2}\iiint_{D} \sigma^0_{ij}u^0_{i,j}\,dV - \iint_{|D|} \sigma^0_{ij}n_ju^0_i\,dS. \tag{30}$$

The change of the potential energy due to the inhomogeneity becomes

$$\Delta W = W - W_0 = \frac{1}{2}\iiint_{\Omega} \sigma_{ij}u^0_{i,j}\,dV - \frac{1}{2}\iiint_{\Omega} \sigma^0_{ij}u_{i,j}\,dV - \frac{1}{2}\iint_{|\Omega|} \sigma^0_{ij}n_j[u_i]\,dS \tag{31}$$

after some calculations. ΔW is therefore expressed by the quantities defined in Ω and $|\Omega|$, and can be easily evaluated.

4. NUMERICAL RESULTS

Numerical examples of stress fields are given. As stated by Tsutsui and Saito[13], the effect of Poisson's ratio difference is negligible in comparison with that of the shear-modulus difference. Therefore, we take various $\Gamma = \bar{G}/G$ but $\nu = \bar{\nu} = 0.3$. In the inclusion problem we take a special case $\Gamma = \bar{G}/G = 1$, and in all graphs $s = a/b = 0.5$ where $a_1 = a_2 = a$ and $a_3 = b$. Results are compared with the perfect-bonding case. The most essential difference between the solution for the sliding inhomogeneity (or inclusion) and that for the perfect-bonding inhomogeneity (or inclusion) is that the infinite series are necessary for the solution for the sliding case, but finite series with $n = 5$ are enough for the perfect-bonding case. The infinite system of algebraic equations for A_n, B_n, $\bar{A}_n$, $\bar{B}_n$ is truncated to $n = 15$. This approximation is accurate enough to show three significant figures in the included numerical examples. After the coefficients are determined, we can compute the stresses and the displacements at any point in the space or in the inhomogeneity (or inclusion).

Figures 2–6 present the variation of $\bar{\sigma}_x$, $\bar{\sigma}_y$ and $\bar{\sigma}_z$ with ϕ (see Fig. 1) along the interface between the matrix and the inhomogeneity or inclusion for both the slip (solid lines) and the perfect-bonding (dashed lines) cases. The value of ϕ is obtained from β by the eqn $\tan\phi = (a/b)\tan\beta$.

Figures 2 (hard particle) and 3 (soft particle) are for the all-around tension at infinity; figs. 4 and 5 are for the transversal and longitudinal eigenstrains, respectively. Figure 6 is for the uniaxial tension at infinity. In each case γ is taken as 90°.

We can see that the stresses for the slip conditions are not constant in the inclusion or the inhomogeneity. Recall that for the perfect-bonding case, stresses are constant as discovered by Eshelby[5]. When the inhomogeneity is under all-around tension at infinity, the highest tensile stress in the inhomogeneity occurs at $\phi = 90°$, and a large

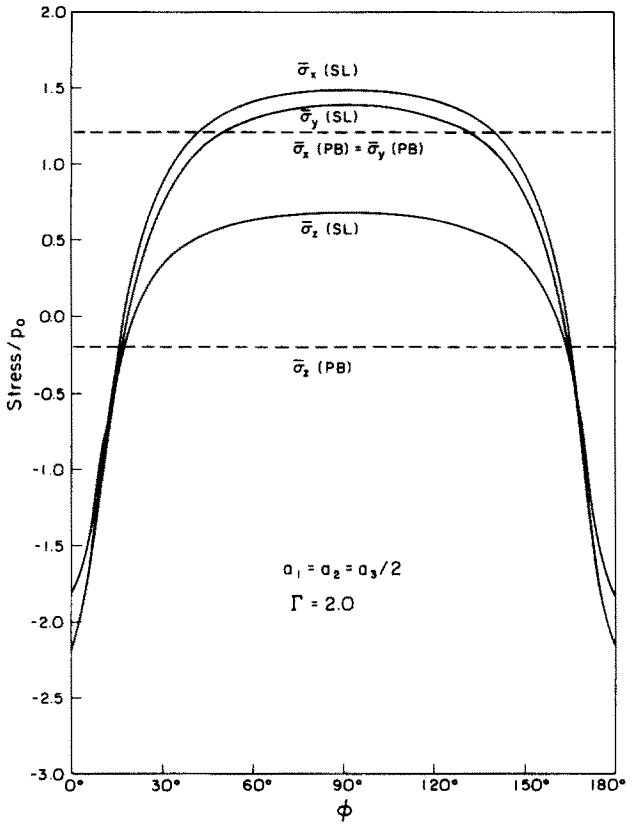

Fig. 2. Variation of $\bar{\sigma}_x$, $\bar{\sigma}_y$ and $\bar{\sigma}_z$ (caused by all-around tension p_0) in the inhomogeneity on the spheroidal interface with ϕ for $s = a/b = 0.5$, $\Gamma = \bar{G}/G = 2.0$, $\nu = \bar{\nu} = 0.3$ and $\gamma = \pi/2$.

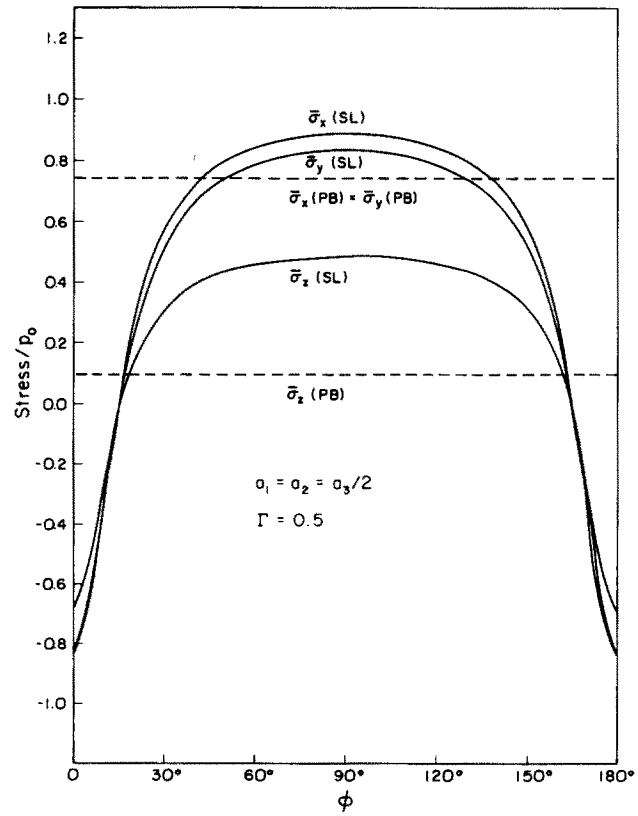

Fig. 3. Variation of $\bar{\sigma}_x$, $\bar{\sigma}_y$ and $\bar{\sigma}_z$ (caused by all-around tension p_0) in the inhomogeneity on the spheroidal interface with ϕ for $s = 0.5$, $\Gamma = 0.5$ and $\gamma = \pi/2$.

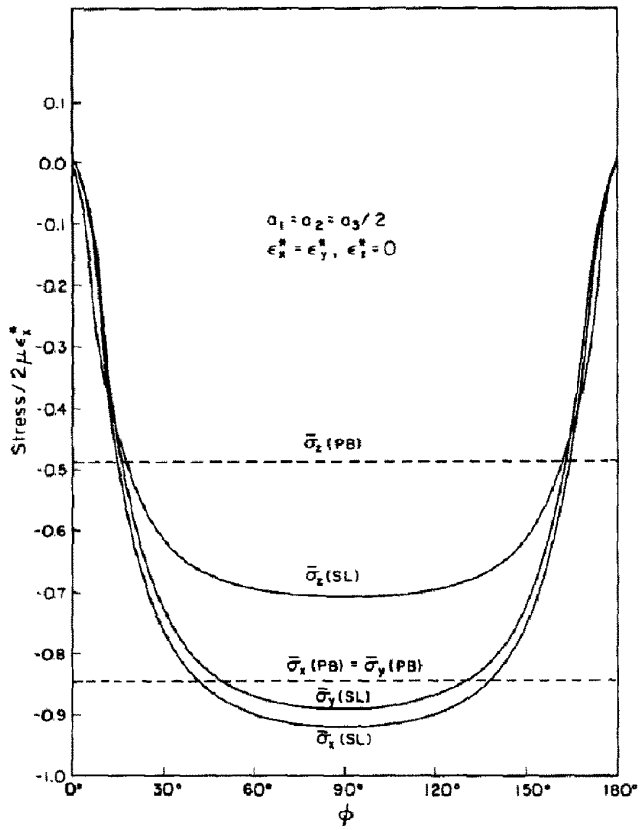

Fig. 4. Variation of $\bar{\sigma}_x$, $\bar{\sigma}_y$ and $\bar{\sigma}_z$ (caused by $\epsilon_x^* = \epsilon_y^*$, $\epsilon_z^* = 0$) in the inclusion on the spheroidal interface with ϕ for $s = 0.5$, $\Gamma = 1$ and $\gamma = \pi/2$.

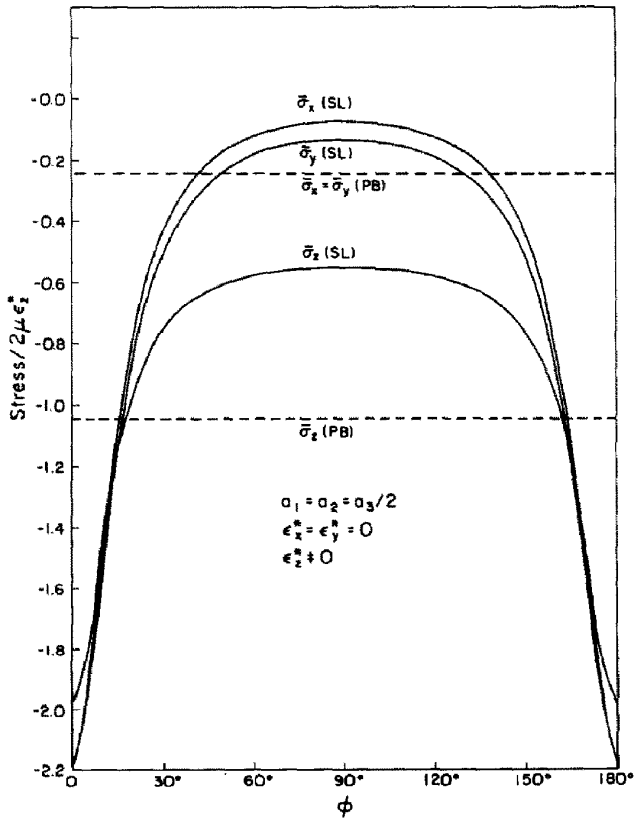

Fig. 5. Variation of $\bar{\sigma}_x$, $\bar{\sigma}_y$ and $\bar{\sigma}_z$ (caused by $\epsilon_x^* = \epsilon_y^* = 0$, $\epsilon_z^* \neq 0$) in the inclusion on the spheroidal interface with ϕ for $s = 0.5$, $\Gamma = 1$ and $\gamma = \pi/2$.

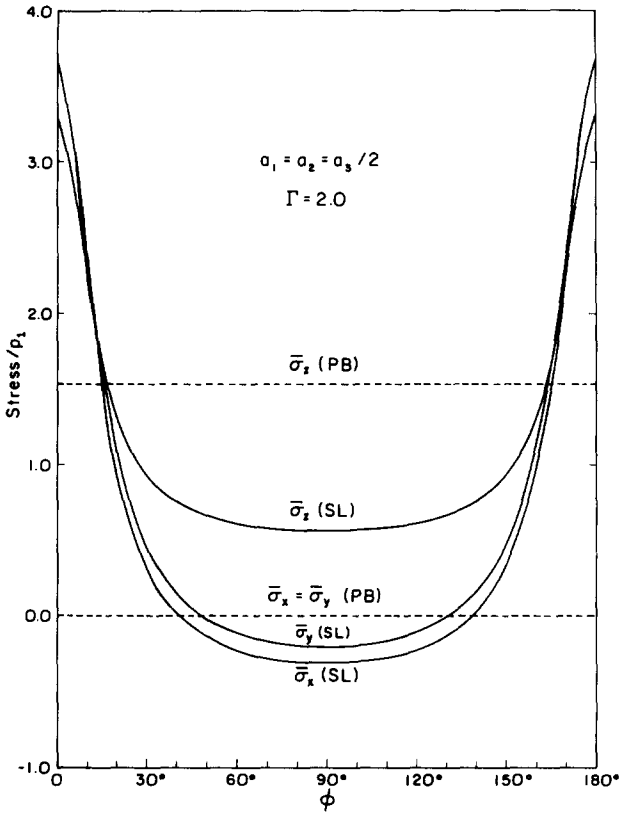

Fig. 6. Variation of $\bar{\sigma}_x$, $\bar{\sigma}_y$ and $\bar{\sigma}_z$ in the inhomogeneity along the z-axis for $s = 0.5$ and $\Gamma = 0.5$.

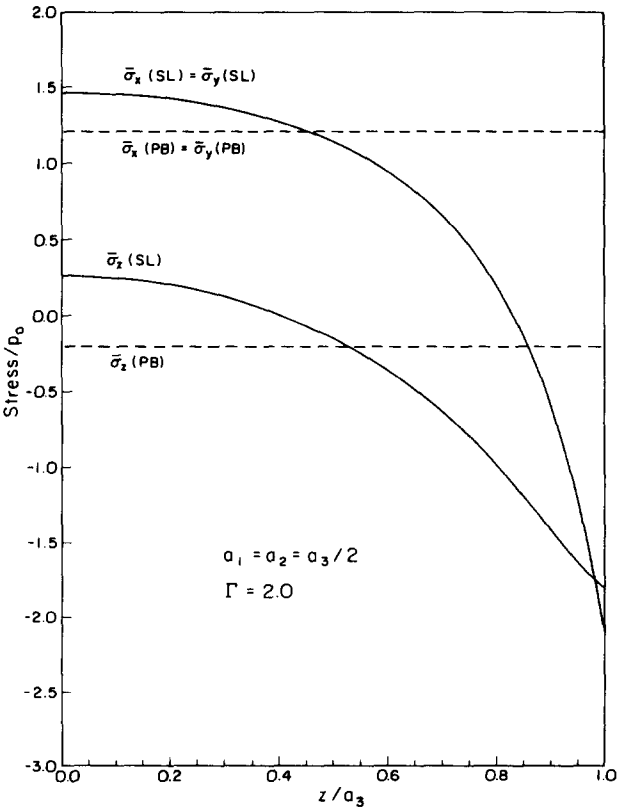

Fig. 7. Variation of $\bar{\sigma}_x$, $\bar{\sigma}_y$ and $\bar{\sigma}_z$ in the inhomogeneity along the z-axis for $s = 0.5$ and $\Gamma = 2.0$.

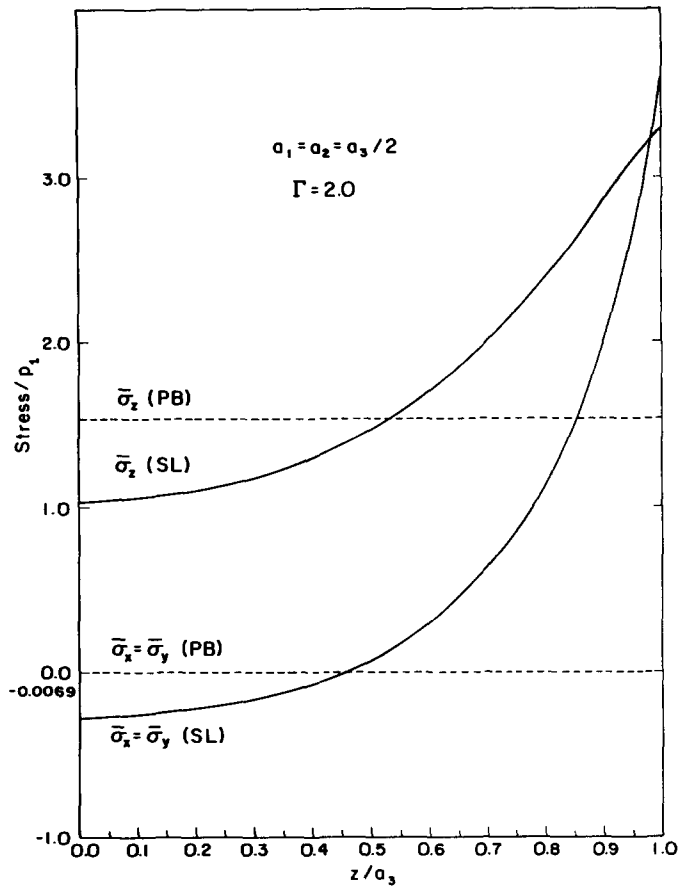

Fig. 8. Variation of $\bar{\sigma}_x$, $\bar{\sigma}_y$ and $\bar{\sigma}_z$ in the inhomogeneity along the z-axis for $s = 0.5$, $\epsilon_x^* = \epsilon_y^*$, $\epsilon_z^* = 0$ and $\Gamma = 2.0$.

compression is caused at $\phi = 0°$ and 180°. When the inhomogeneity is under uniaxial tension at infinity, the large tensile stress in the inhomogeneity occurs at $\phi = 0°$ and 180°, and minimum is at $\phi = 90°$. It is observed that for both cases the tensile and compressive stresses are higher for the hard inclusion ($\Gamma > 1$). When the eigenstrains are present, both the perfect inclusion and the sliding inclusion are under compressive stresses everywhere. The stress distribution for the sliding inclusion varies and the highest compressive stress exceeds the one in the perfect-bond state. The average stress, however, decreases due to sliding. This is seen from Table 2 since the average stress is proportional to the elastic energy as shown in the last section. Therefore, according to the self-consistent concept, the effect of sliding depresses the average elastic moduli of composite materials.

Figures 7–10 show the variations of $\bar{\sigma}_x$, $\bar{\sigma}_y$ and $\bar{\sigma}_z$ along the z-axis, for $s = 0.5$. The maximum compressive stress appears at the center for the transversal eigenstrain and at the end (north and south poles) for the longitudinal eigenstrain.

Figure 11 presents σ_x, σ_y and σ_z along the interface in the matrix when the inhomogeneity is under all-around tension at infinity. The maximum compression stresses

Table 2. The elastic energy of the inclusion for the perfect bonding and the slip case, ($s = 0.5$, $\Gamma = 1$)

	Perfect inclusion	Sliding inclusion	Relaxation percentage
I. $\epsilon_x^* = \epsilon_y^* \neq 0$, $\epsilon_z^* = 0$	0.845731	0.815436	3.7
II. $\epsilon_x^* = \epsilon_y^* = 0$, $\epsilon_z^* \neq 0$	0.5233975	0.405653	29.0
III. $\epsilon_x^* = \epsilon_y^* = \epsilon_z^* \neq 0$.	1.857143	1.801363	3.1

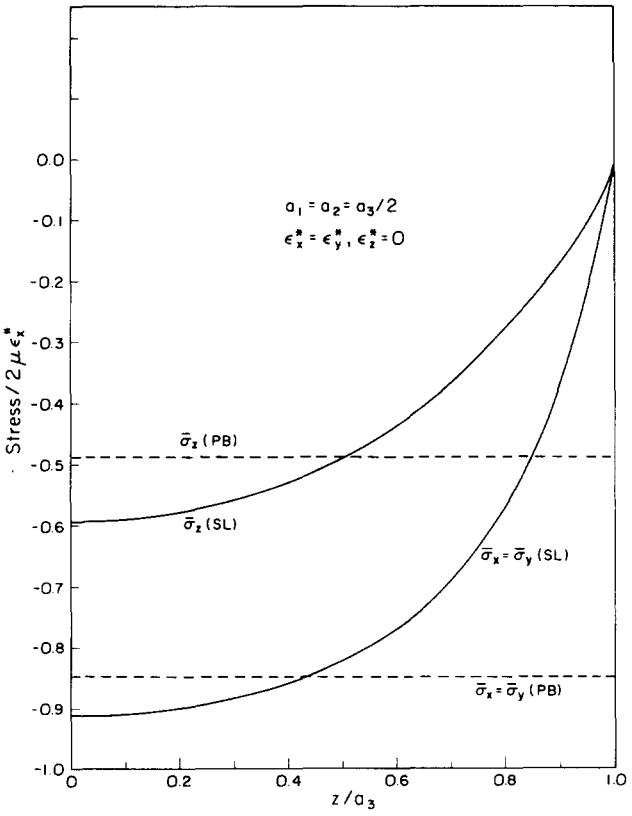

Fig. 9. Variation of $\bar{\sigma}_x$, $\bar{\sigma}_y$ and $\bar{\sigma}_z$ in the inclusion along the z-axis for $s = 0.5$, $\epsilon_x^* = \epsilon_y^* \neq 0$, $\epsilon_z^* = 0$ and $\Gamma = 1$.

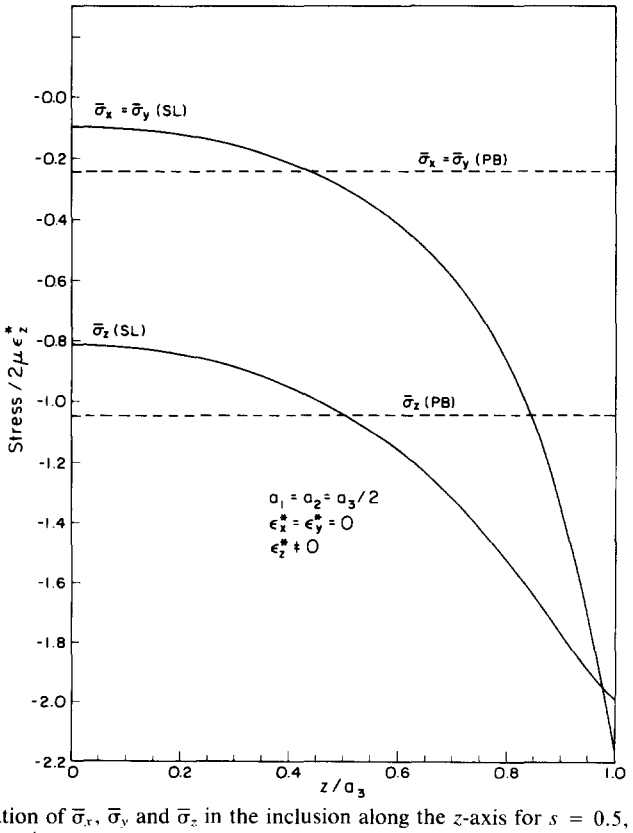

Fig. 10. Variation of $\bar{\sigma}_x$, $\bar{\sigma}_y$ and $\bar{\sigma}_z$ in the inclusion along the z-axis for $s = 0.5$, $\epsilon_x^* = \epsilon_y^* = 0$, $\epsilon_z^* \neq 0$ and $\Gamma = 1$.

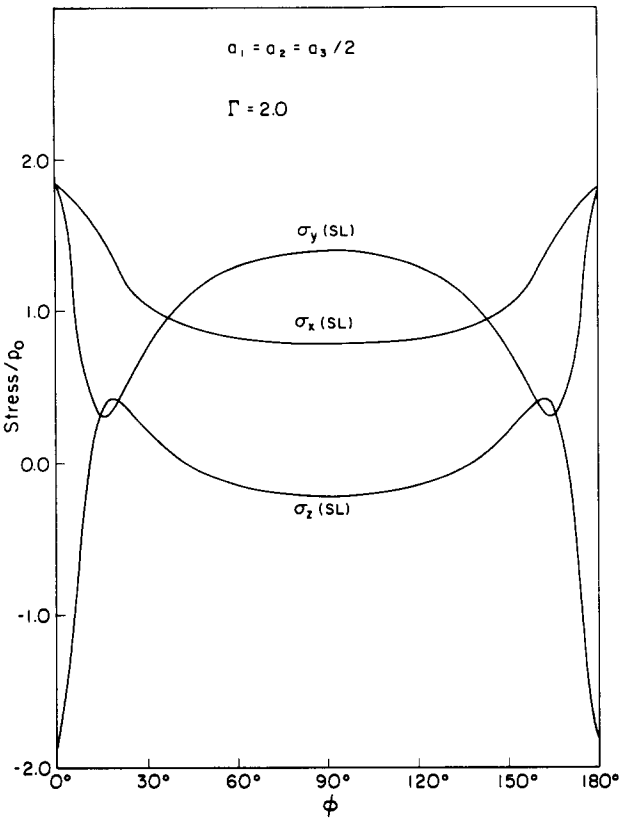

Fig. 11. Variation of σ_x, σ_y and σ_z in the matrix on the spheroidal interface with ϕ caused by all-around tension p_0 for $s = 0.5$, $\Gamma = 2.0$ and $\gamma = \pi/2$.

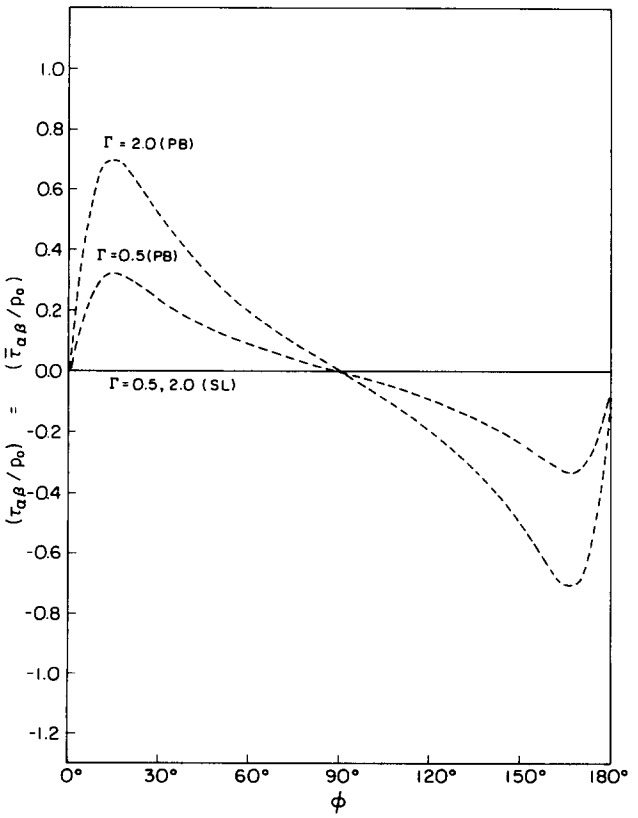

Fig. 12. Variation of $(\tau_{\alpha\beta})_{\alpha=\alpha_0} = (\bar{\tau}_{\alpha\beta})_{\alpha=\alpha_0}$ under p_0 in the inhomogeneity on the spheroidal interface with ϕ for $s = 0.5$ and $\Gamma = 0.5, 2.0$.

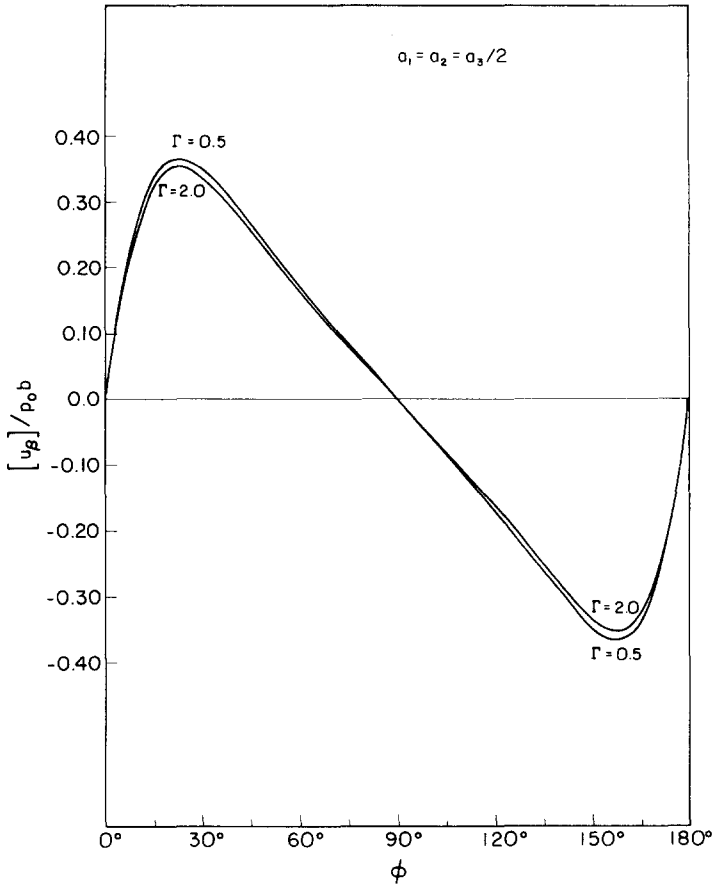

Fig. 13. Sliding $[u_\beta]$ along the interface caused by p_0.

are in the matrix at $z = \pm b$, i.e. when $\phi = 0°$ or 180°. The discontinuity of σ_x component is seen at $\phi = 90°$, compared with $\bar{\sigma}_x$ at $\phi = 90°$ in Fig. 2, where $\gamma = 90°$.

Figure 12 shows the variation of $(\bar{\tau}_{\alpha\beta})_{\alpha=\alpha_0} = (\tau_{\alpha\beta})_{\alpha=\alpha_0}$ along the interface for the perfect-bonding (dashed lines) and slip (solid line) cases. It can be seen that for the perfect-bonding case the shear stress varies along the interface and becomes zero only at $\phi = 0°$, 90° and 180°, while it is zero everywhere for the slip case.

Figure 13 shows the relative sliding along the interface for all-around tension case. From Figs. 12 and 13 it can be seen that the sliding is caused by the relaxation of the tangential shear stress present in the perfect-bonding case.

Table 2 shows the numerical comparison between the elastic energy in the perfectly bonded and sliding inclusions. Note that the elastic energy is lower for the sliding case. We conclude, therefore, that the sliding along the interface causes a relaxation even though the absolute value of stress increases locally, and depresses the average elastic moduli.

5. CONCLUSION

In this paper we presented a method of solution for the prolate spheroidal inclusion contained in an infinite elastic material subjected to a constant nonshear eigenstrain and the inhomogeneity of the same shape under all-around tension or uniaxial tension at infinity.

The numerical results for the slip boundary condition were compared with the perfect-bonding case. We concluded that when the shear traction is specified to vanish along the boundary, none of the stress components in the inhomogeneity or the inclusion are constant, contrary to the perfect-bonding case, where the Eshelby solution holds.

Although the solution for the perfect-bonding case is expressed by the finite series, the solution for the sliding case requires infinite series. However, when the inclusion or inhomogeneity has the shape of a sphere, the sliding solution is degenerated into the finite series as expected from the solution of Ghahremani[11].

The elastic energy in the sliding inclusion is lower than in the perfectly bonded inclusion. We conclude, therefore, that sliding along the interface causes the stress relaxation in the inclusion even though the absolute value of stress increases locally.

Acknowledgements—This research was supported by the U.S. Army Grant No. DAAG29-81-k-0090.

REFERENCES

1. J. N. Goodier, *J. Appl. Mech.* **57,** 39 (1933).
2. M. A. Sadowsky and E. Sternberg, *J. Appl. Mech.* **69,** A191 (1947).
3. H. Miyamoto, *J. Jpn. Soc. Appl. Mech.* **3,** 15 (1950).
4. R. H. Edwards, *J. Appl. Mech.* **18,** 19 (1951).
5. J. D. Eshelby, *Proc. Roy. Soc.* **A241,** 376 (1957).
6. J. D. Eshelby, *Proc. Roy. Soc.* **A252,** 561 (1959).
7. L. J. Walpole, *Proc. Roy. Soc.* **A300,** 270 (1967).
8. N. Kinoshita and T. Mura, *Phys. Status Solidi (a)* **5,** 759 (1971).
9. R. J. Asaro and D. M. Barnett, *J. Mech. Phys. Solids* **23,** 77 (1975).
10. T. Mura and R. Furuhashi, *J. Appl. Mech.* **51,** 308 (1984).
11. F. Ghahremani, *Int. J. Solids Structures* **16,** 825 (1980).
12. E. Tsuchida and T. Mura, *J. Appl. Mech.* **50,** 807 (1983).
13. S. Tsutsui and K. Saito, *Proc. 23rd Jpn. Nat. Congr. Appl. Mech.* **23,** 547 (1973).